Journal of the Serbian Society for Computational Mechanics / Vol. 19 / No. 2, 2025 / pp 106-115 / original paper
(10.24874/jsscm.2025.19.02.07)

FAULT DETECTION USING RADIOSENSOR DIAGNOSTICS

Konstantin A. Boikov [0000-0003-0213-7337]

MIREA - Russian Technological University, Moscow, Russia
e-mail: nauchnyi@yandex.ru

Abstract

The purpose of this paper is to increase the efficiency of determining the technical condition of complex electronic devices by recording and analyzing electromagnetic fields induced by signal emissions from elements of their printed topology. We used experimental research methods to receive and record the electrical component of the electromagnetic field emitted by the product - a signal radio profile (SRP). The results showed the possibility of detecting a malfunction when analyzing the correlation function between the benchmark and the adopted SRP, which determines the novelty of the work. It has been established that when the correlation coefficient between the studied SRP and the reference point is less than 0.9, the fault can be not only detected, but also localized. Using the example of an element of the Smart Home system - a heating controller with intentionally introduced faults into its relay control unit, the possibility of identifying and localizing a fault at an early stage of its occurrence is shown. The practical significance of the paper lies in the possibility of determining a malfunction using the radiosensor diagnostics (RSD) method at an early stage, which is not available to other methods for determining the technical condition.

Keywords: fault detection, signal radio profile, correlation analysis, time-frequency decomposition, spurious emissions, determination of technical condition.

1. Introduction

Radio-electronic equipment (REE), which allows for remote communication with infrastructure objects (control, monitoring, management), is rapidly developing and covers many areas of human activity. Systems such as “Smart Home”, “IoT” and their elements - heating, ventilation, humidification, alarm controllers have now become widely available to users in the household sector (Bharti and Kapoor, 2020). Not only the comfort and safety of the property of the average user, but also environmental control, sustainable production and economic security depend on the stable functioning of such hardware and software communication systems. Continuously increasing demands on the reliability of electronic distribution systems require the effective search and development of new methods of technical diagnostics (TD). Known scientific methods for assessing the technical condition require physical access to possible places where faults occur, and also stop the operation of the electronic distribution system, which is often unacceptable and significantly complicates maintenance (Boikov, 2021).

These conditions lead to the need for developing and improving TD methods that are independent of the complexity and architecture of radio-electronic nodes of electronic distribution systems, which determines the relevance of the paper.

The purpose of this paper is to increase the efficiency of determining the technical condition of complex electronic devices and to demonstrate the detection of malfunctions in the heating controller (an element of the Smart Home system) using a new method of radiosensory technical diagnostics (RTD), carried out by recording and analyzing electromagnetic fields induced by signal emissions of printed topology elements REE.

The method of RTD is just beginning to develop, its description and research in the literature is almost never found. The paper by Kostin (2024) presents the main ideas of the method of radiosensory diagnostics and identification of REE.

2. Materials and methods

To carry out RTD, it is necessary to register a signal radio profile – the electrical component of the electromagnetic field emitted by the electronic components of the REE. This radiation for digital electronic devices is possible at the moments of power supply, clocking, access to the periphery, and changes in power consumption modes (Boikov, Kostin and Kulikov, 2021). For analogue REE, registration of SRP is possible only at the moment of supplying the supply voltage.

In the paper by Boikov (2022), it is shown that the general SRP is a linear superposition of the SRP of the input and output circuits of its components, emitting free damped oscillations:

$$U(t)=\sum_{i=1}^{N}U_{CBi}(t)=\sum_{i=1}^{N}U_{0i}e^{-\delta_i(t-t_{0i})}\sin\left[\omega_i(t-t_{0i})\right] \tag{1}$$

where U_{CB} is the instantaneous value of the reduced level of the i-th oscillation, U_0 is the reduced amplitude of the first half-wave of the i-th oscillation, δ is the attenuation coefficient of the i-th oscillation, t is the current moment in time, t_0 is the time of the start of radiation of the i-th oscillation, f – frequency of the i-th oscillation, $\underline{N}$ – number of emitters. (Here are described the parameters of the emitters presented in Tables 1-3).

Analytical expression (1) is the main one for the SRP, since it contains the correspondence of the change in the nature of the time-frequency dependence of the SRP with changes in the radio technical parameters of the studied REE.

Fig. 1 shows an approximate SRP and its components – damped oscillations corresponding to certain REE emitters.

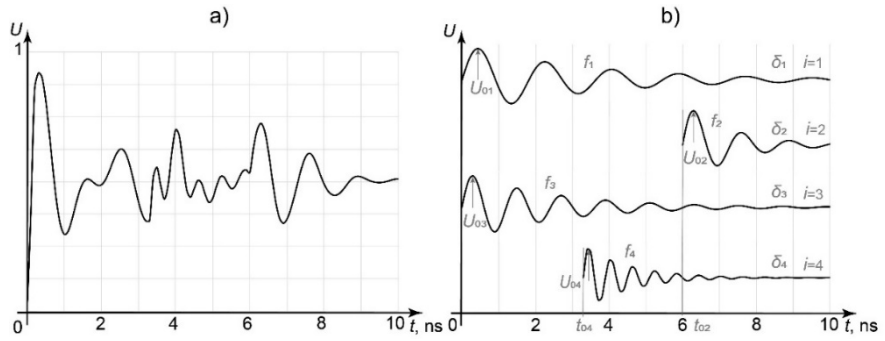

Fig. 1. SRP: a) superposition of radiation; b) signal components

As it can be seen from the figure, the SRP consists of four emitters, the presence of which is due to parasitic energy storage devices in the input and output circuits of the REE.

To decompose the SRP into simple damped oscillations, determining their number and extracting the main parameters, it is necessary to decompose it (Porsani, Silva and Ursin, 2019), through a time-frequency transformation.

$$X(f,h)=\sum_{h=0}^{K-O}\left[\sum_{c=h}^{O-1+h}U(O)\exp\left(-j\frac{2\pi fc}{O}\right)\right] \tag{2}$$

where *X(f, h)* is the discrete time-frequency spectrum of the signal, *h* is the sample number of the position of the conversion window ($0 < h <$ K - O), *K* is the total number of SRP samples, *U(O)* is the signal sampled in time, *c* – sample number, *f* – frequency, *O* – number of points forming the transformation window.

The transformation window in expression (2) is understood as a rectangular function *O(t)*, which moves along the time axis from the origin (Shevgunov and Gushchina, 2021), the window width is the number of sampling points falling into the rectangular window function, the window step is the number of sampling points to which moves rectangular window function:

$$O(t)=\begin{cases}1, & t\le|t_O|\\ 0, & t>|t_O|\end{cases}$$

To record SRP, it is enough to have a measuring antenna, a low-noise amplifier and an ultra-fast real-time oscilloscope. Fig. 2 shows a block diagram of a measuring stand for receiving SRP.

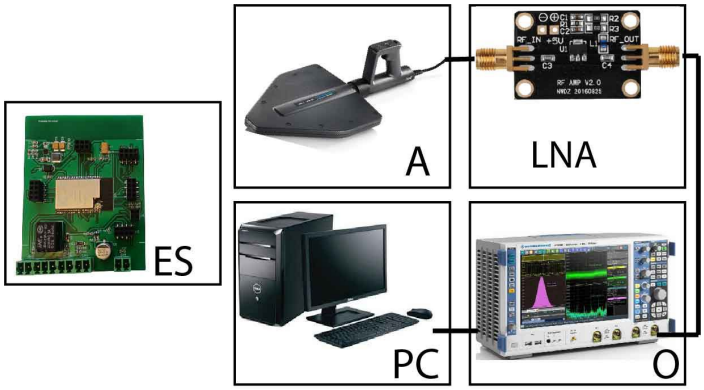

Fig. 2. Block diagram of the measuring stand

In this figure: **ES** – experimental sample, **A** – broadband antenna, **LNA** – low-noise broadband amplifier, **PC** – personal computer, **O** – ultra-high-speed real-time oscilloscope.

The radiation is received in the near field at a distance of no more than ten centimeters from the sample under study, so that the elements of the measuring stand do not affect the formation of the SRP. Each element of the measuring stand is subject to certain requirements in terms of bandwidth, speed and sampling parameters. The wider the frequency band under study, the more detailed the SRP can be analyzed. Research shows that for an average SRP length of 5 – 100 ns, the components of the measuring stand should be selected with a frequency range of at least 0.1 – 5 GHz, a sampling frequency of at least 10 GS/s, and a resolution of at least 10 bits.

To recognize faults, it is necessary to study the deviation of the reference SRP obtained from a known functional REE and the SRP received from a faulty sample. The study is carried out by the method of correlation analysis of the obtained and original SRP by constructing the correlation function *r(h)*:

$$r(h)=\frac{\sum_{i=h}^{M+h}\left(Y_{1,i}-\bar{Y}_1\right)\cdot\left(Y_{2,i}-\bar{Y}_2\right)}{\sqrt{\sum_{i=h}^{M+h}\left(Y_{1,i}-\bar{Y}_1\right)^2\cdot\sum_{i=h}^{M+h}\left(Y_{2,i}-\bar{Y}_2\right)^2}} \tag{3}$$

where M is the number of samples (“transformation window”), h is the number of the “window” position sample *(0 < h < K - M)*, K is the total number of SRP samples, $Y_1=\frac{U}{U_M}$ is a sample of SRP values *a*, $Y_2=\frac{U_B}{U_{MB}}$ – is a sample of SRP values *б*, $\bar{Y}_1=\frac{1}{M}\sum_{i=h}^{M+h}Y_{1,i}$, $\bar{Y}_2=\frac{1}{M}\sum_{i=h}^{M+h}Y_{2,i}$ is the mean value of the samples, U is the value of SRP a at the sampling point, U_M is the maximum value of SRP a, U_B is the value of SRP b at the sampling point, U_{MB} is the maximum value of SRP b.

For the study, we will take the motherboard of the heating controller (Fig. 3a) and simulate damage to the control relay winding. If it fails, the correct functioning of the entire controller as a whole is impossible. Fig. 3b shows the electrical circuit diagram of the relay block switching.

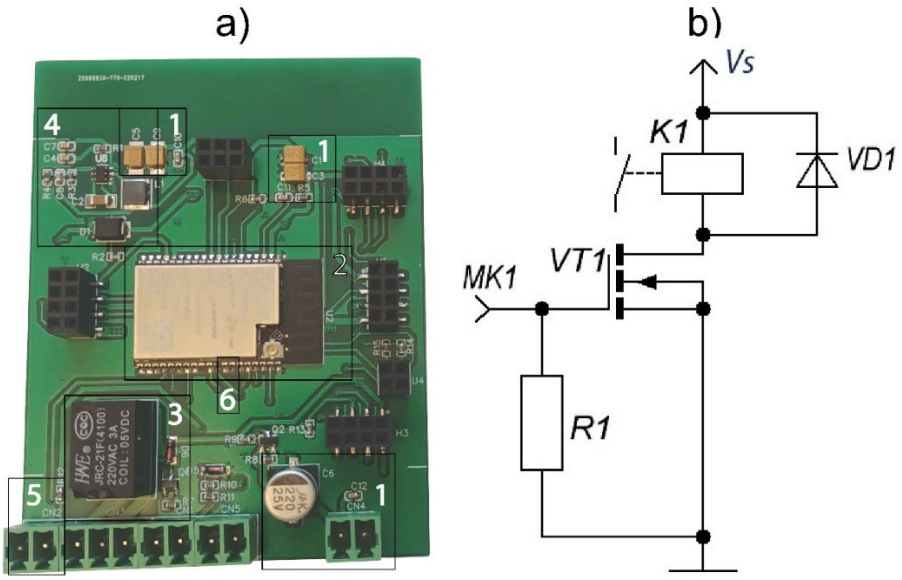

Fig. 3. Heating controller: a) motherboard, b) relay unit

In the presented figure: 1 – high-quality power supply capacitances, 2 – microcontroller, 3 – control relay, 4 – pulse step-down voltage converter, 5 – temperature sensor input, 6 – reading an analog-to-digital converter, *MK1* – control output from the controller, *R1* – pull-up resistor, *K1* – relay, *VT1* – key MOSFET, *VD1* – protective diode.

RTD for complex devices is impossible without the use of a computer, since the number of nodes under study can reach tens, and the decomposition parameters can reach several hundred. Therefore, the analysis of the adopted SRP will be carried out in specially developed software (Boikov and Shamin, 2022).

3. Results

As a result, a reference SRP was obtained, which was necessary for the correct implementation of RTD. Fig. 4 shows the reference SRP for launching the heating controller motherboard with decomposition into its components.

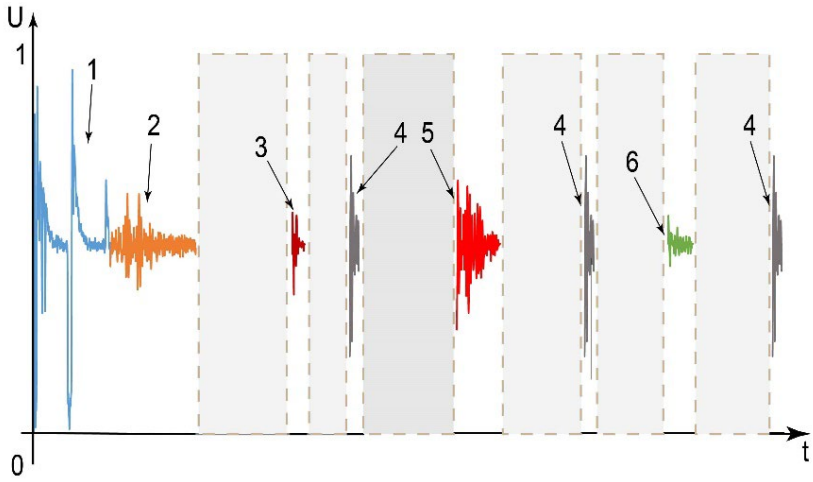

Fig. 4. SRP for starting the motherboard (1 – high-quality power supply capacitors, 2 – microcontroller, 3 – control relay, 4 – pulse step-down voltage converter, 5 – temperature sensor input, 6 – reading analog-to-digital converter).

These SRP components were obtained for each functional block separately. The simplest option for localizing a fault is the absence of unit emitters, which will indicate a unit that is not performing its function.

However, in practice, there are often malfunctions that do not lead to a complete absence of radiation. For example, consider damage to the winding of the control relay (Fig. 4, SRP-3). If it fails, the correct functioning of the entire heating controller is impossible. Fig. 5 shows sections of the adopted SRP and benchmark.

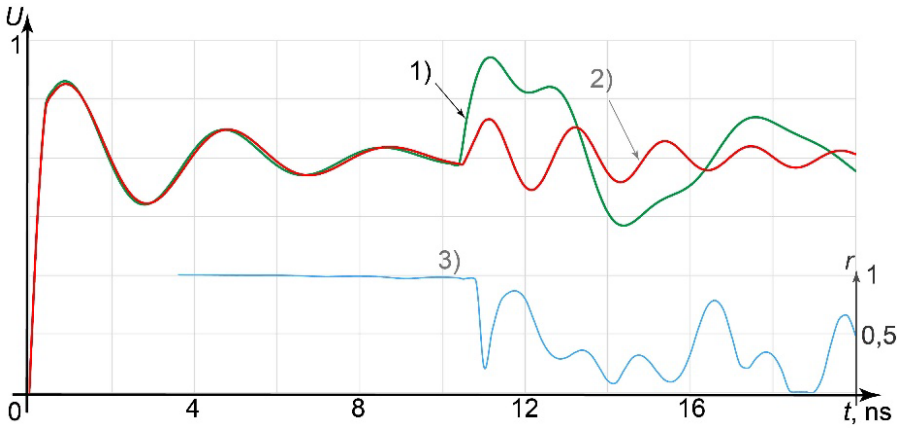

Fig. 5. SRP: 1 – reference point, 2 – accepted SRP, 3 – correlation function

For a more detailed study of the malfunction, the parameters of the SRP were extracted during its decomposition.

Emitters	f, GHz	δ, nc^{-1}	t_0, nc	U_0
Benchmark				
i=1	0,52	-0,52	0	0,83
i=2	0,33	-0,30	10,5	0,97
i=3	0,93	-0,60	10,5	0,40
Accepted SRP				
i=1	0,50	-0,50	0	0,80
i=2	-	-	-	-
i=3	0,92	-0,62	10,4	0,42

Table 1. SRP parameters when the relay coil breaks.

Also, one of the possible malfunctions is a short circuit in the output circuit of the switching MOSFET (breakdown of the protective diode VD1). Fig. 6 shows sections of the accepted SRP during a short circuit in comparison with the reference.

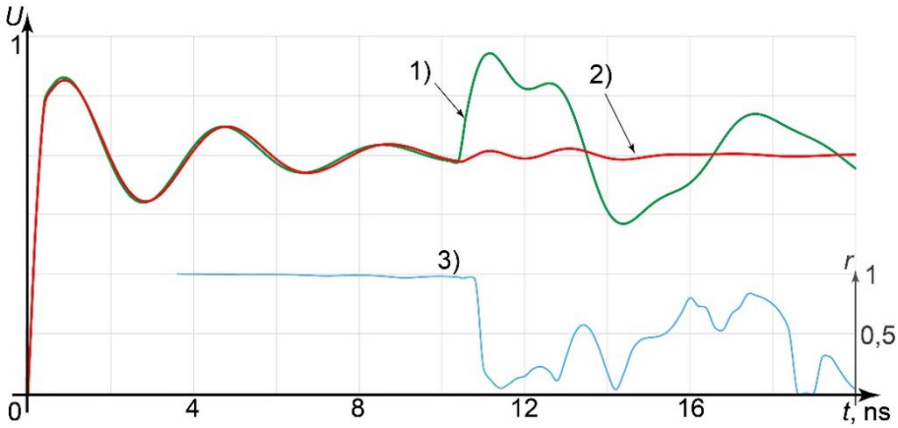

Fig. 6. Breakdown of the protective diode VD1: 1 – reference point, 2 – accepted SRP, 3 – correlation function.

Table 2 presents the extracted SRP parameters.

Emitters	f, GHz	δ, nc^{-1}	t_0, nc	U_0
Benchmark				
i=1	0,52	-0,52	0	0,83
i=2	0,33	-0,30	10,5	0,97
i=3	0,93	-0,60	10,5	0,40
Accepted SRP				
i=1	0,50	-0,50	0	0,80
i=2	-	-	-	-
i=3	-	-	-	-

Table 2. SRP parameters during breakdown of the protective diode.

The most difficult problem is the degradation of the gate dielectric in MOSFETs, which arises during operation. Fig. 7 shows the SRP obtained from a MOSFET degraded as a result of incorrect temperature conditions in comparison with the reference.

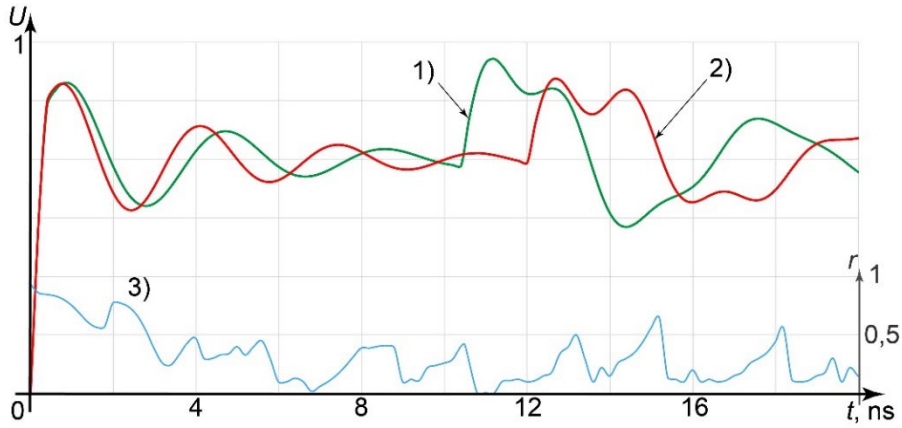

Fig. 7. Gate dielectric degradation: 1 – reference point, 2 – accepted SRP, 3 – correlation function.

To study the consequences of this degradation in more detail, SRP parameters were extracted.

Emitters	f, GHz	δ, nc^{-1}	t_0, nc	U_0
Benchmark				
i=1	0,52	-0,52	0	0,83
i=2	0,33	-0,30	10,5	0,97
i=3	0,93	-0,60	10,5	0,40
Accepted SRP				
i=1	0,61	-0,49	0	0,80
i=2	0,31	-0,27	12,0	0,93
i=3	0,92	-0,62	12,0	0,42

Table 3. Parameters of SRP during gate dielectric degradation.

4. Conclusions

As it can be seen from Fig. 5, the elementary emitter connected to the output circuit of the MOSFET VT1 (break in the load) has disappeared from the SRP with a malfunction (damage to the winding of the control relay). The relay winding is broken, and the radiation associated with it is absent. Therefore, there is no data in line i=2 in Table 1. This can be seen in Table 1, which shows the decomposition of the SRP into components, according to expression (1). The parameters in the table are described in detail in expression 1. In the adopted SRP, the second emitter is missing (i = 2), while the remaining SRP parameters have remained virtually unchanged. This fact leads to a sharp decrease in the correlation coefficient, which is subsequently recorded by special software, informing the operator about the occurrence of an abnormal situation when starting the heating controller.

Fig. 6 shows how the correlation function drops off sharply in the region of the emitter connected to the output circuit. This occurs as a result of the protective diode shunting the entire output circuit and neutralizing the output emitter. The protective diode shunts the circuit of the output emitter of the transistor VT1 (i=3) and the coil of the relay K1 (i=2). This completely blocks the output circuit emissions since there is no oscillatory circuit. When decomposed in Table 2, the absence of emitters (i = 2, i = 3) associated with the output circuit is noticeable, which makes it possible to localize this fault.

As it can be seen from Fig. 7, the correlation function has dips in the region of the radiation-related input and output circuits *VT1*, which is due to changes in the properties of the gate dielectric. Physical or chemical degradation is associated with external factors, such as high temperature, possible humidity, chemically aggressive substances, etc. This may cause the transistor to malfunction or partially fail. Degradation also produces defects, such as traps on the surface of the dielectric, which can affect the flow of charge through the dielectric and change the characteristics of the transistor. The PRD method, unlike currently known functional diagnostic methods, is capable of identifying possible malfunctions associated with the degradation of elements. As a result of changes in the properties of the dielectric, the input and output capacitance of the transistor VT1 changes, which means that the parameters of the oscillatory circuits connected to it change. Table 3 shows changes in the parameters of the emitters in different colors. Table 3 shows that all emitters are present, but degradation has led to a decrease in the MOSFET response time, which is shown by the response time parameter t0,

presented in expression (1) for emitters $i = 2$ and $i = 3$. The input capacitance VT1 has also changed, which is indirectly shown by the frequency parameter f of the first emitter ($i = 1$).

The results presented in this paper enable evaluation of the advantages of the new RTD method for localizing faults even at an early stage of their occurrence. This method, based on the time-frequency analysis of the redistribution of the electromagnetic field of the SRP, induced by the radiation of elements of the printed topology of the electronic distribution network, makes it possible to identify not only software and hardware faults, but also parametric deviations of their radio-electronic components.

RTD can be used as a development and addition to existing methods for complex functional diagnostics of REE. The use of modern ultra-high-speed recording equipment together with special software for determining and decomposing SRP makes it possible to localize faults in complex electronic devices using a non-contact method, included in mass production. An important advantage of the RTD method is the absence of influence of the measuring equipment on the object of study. Also, studying the SRP allows you to detect only an emerging or hidden fault, which cannot be determined by modern TD methods, which opens up new opportunities in the field of determining the technical condition of the electronic distribution system.

References:

Bharti, P. and Kapoor, P. (2020). A survey on applications and challenges of Internet of Things (IoT). Mobile Networks and Applications, 25(12), 4700-4720.

Boikov, K.A. (2021). Determination of the parameters of electronic devices by the method of passive radiosensor technical diagnostics. News of higher educational institutions of Russia. Radioelectronics, 24(6), 63-70. https://doi.org/10.32603/1993-8985-2021-24-6-63-70.

Kostin, M.S. & Boikov K.A. (2024). Digital technologies for signal radio vision and radio monitoring. Russian Technological Journal, 12(4), 59–69. https://doi.org/10.32362/2500-316X-2024-12-4-59-69.

Boikov, K.A. (2022). Radiosensor identification and authentication of radio-electronic devices. T-Comm, 16(5), 15-20. DOI: 10.36724/2072-8735-2022-16-5-15-20

Boikov, K.A., Kostin, M.S. and Kulikov, G.V. (2021). Radiosensory diagnostics of signal integrity in-circuit and peripheral architecture of microprocessor devices. Russian Technological Journal, 9(4), 20-27. https://doi.org/10.32362/2500-316X-2021-9-4-20-27.

Huang, R. and Cui, H. (2015). Consistency of chi-squared test with varying number of classes. Journal of Systems Science and Complexity, 28(2), 439-450. https://doi.org/10.1007/s11424-015-3051-2.

Porsani, M.J., Silva, M.G. and Ursin, B. (2019). Signal decomposition and time-frequency representation using iterative singular spectrum analysis. Geophysical Journal International, 217(2), 748-765. DOI: 10.1093/gji/ggz046

Shevgunov, T.Ya. and Gushchina, O.A. (2021). Using two-dimensional fast Fourier transform for estimating spectral correlation function. T-Comm, 15(11), 54-60. DOI: 10.36724/2072-8735-2021-15-11-54-60

Thanh, T. K. and Vinh, T. T. (2019). The application of correlation function in forecasting stochastic processes. Herald of Advanced Information Technology, 2(4), 268-277. https://doi.org/10.15276/hait04.2019.3.